



MoS₂ Nanosheets Assembled on Three-Way Nitrogen-Doped Carbon Tubes for Photocatalytic Water Splitting

Yujia Zhang[†], Yan Liu[†], Wen Gao, Ping Chen, Hongyu Cui, Yanfei Fan, Xifeng Shi, Yingqiang Zhao, Guanwei Cui* and Bo Tang*

Key Laboratory of Molecular and Nano Probes, Ministry of Education, Shandong Provincial Key Laboratory of Clean Production of Fine Chemicals, College of Chemistry, Chemical Engineering and Materials Science, Collaborative Innovation Centre of Functionalized Probes for Chemical Imaging in Universities of Shandong, Shandong Normal University, Jinan, China

OPEN ACCESS

Edited by:

Wee-Jun Ong,
Xiamen University, Malaysia, Malaysia

Reviewed by:

Kangle Lv,
South-Central University for
Nationalities, China
Hui Pan,
University of Macau, China
Junhua Hu,
Zhengzhou University, China

*Correspondence:

Guanwei Cui
cuiguanwei77@163.com
Bo Tang
tangb@sdu.edu.cn

[†]These authors have contributed
equally to this work

Specialty section:

This article was submitted to
Catalysis and Photocatalysis,
a section of the journal
Frontiers in Chemistry

Received: 24 January 2019

Accepted: 23 April 2019

Published: 17 May 2019

Citation:

Zhang Y, Liu Y, Gao W, Chen P, Cui H,
Fan Y, Shi X, Zhao Y, Cui G and Tang B
(2019) MoS₂ Nanosheets Assembled
on Three-Way Nitrogen-Doped
Carbon Tubes for Photocatalytic
Water Splitting. *Front. Chem.* 7:325.
doi: 10.3389/fchem.2019.00325

In this work, a micron-sized three-way nitrogen-doped carbon tube covered with MoS₂ nanosheets (TNCT@MoS₂) was synthesized and applied in photocatalytic water splitting without any sacrificial agents for the first time. The micron-sized three-way nitrogen-doped carbon tube (TNCT) was facilely synthesized by the calcination of commercial sponge. The MoS₂ nanosheets were assembled on the carbon tubes by a hydrothermal method. Compared with MoS₂, the TNCT@MoS₂ heterostructures showed higher H₂ evolution rate, which was ascribed to the improved charge separation efficiency and the increased active sites afforded by the TNCT.

Keywords: photocatalysis, MoS₂, three-way nitrogen-doped carbon tubes, hydrogen evolution, water splitting

INTRODUCTION

Photocatalytic water splitting is one of the promising strategies to address the global energy and environmental problems (Hinnemann et al., 2005; Dong et al., 2013; Jiang et al., 2013; Chang et al., 2014; Pan et al., 2016; Wang et al., 2016; Anna et al., 2018; Chen et al., 2018; Zeng et al., 2018). TiO₂ is the most investigated material in the semiconductor photocatalysis research field. However, due to the wide bandgap, it is only responsive to UV light, which greatly limits its photocatalytic efficiency (Cui et al., 2013; Shi et al., 2018). In recent years, many visible-light-driven semiconductors have been designed and applied in solar energy conversion research fields (Wang et al., 2014; Pan, 2016; Shao et al., 2017, 2018; Cheng et al., 2018, 2019; Marchal et al., 2018; Wolff et al., 2018; Yang et al., 2019). Molybdenum disulfide (MoS₂) is one of the most attractive materials. As a graphene-like hexagonal material with close-packed layered structure, MoS₂ has a sandwich architecture, in which the strong covalent bonds among S-Mo-S atoms lies in the layer while the weak van der Waals force exists between the layers (Cheiwchanchamnangij and Lambrecht, 2012). With the variable atomic coordination and the electronic structure, MoS₂ exhibits extremely fast carriers mobility (over 200 cm²·V⁻¹·s⁻¹). Furthermore, the band gap is adjustable from 1.19 to 1.80 eV through the variation of layer thickness, nanometer size and ion doping. Hence, MoS₂ is an excellent light absorbing material and has high utilization of sunlight. Additionally, the nano-scale molybdenum disulfide has a complicated edge structure with high unsaturation and high reactivity (Wang et al., 2018). In a word, MoS₂ has optimal band gap, high reactive spots and fast mobility of charge carriers, which is beneficial for the photocatalysis. However, the photocatalytic efficiency of pure MoS₂ is still limited by the fast recombination of photogenerated carriers. The construction

of heterostructure of nano-sized MoS₂ coupled with other semiconductor or carbon materials has attracted great interest (Xiang et al., 2012; Jia et al., 2013; Guo et al., 2015; Lang et al., 2015; Pan et al., 2016). It was proposed that the hybrids could provide appropriate band structure for water splitting and improve the separation efficiency of photogenerated carriers.

Herein, MoS₂ nanosheets assembled on a micron-sized three-way nitrogen-doped carbon tube (TNCT@MoS₂) was synthesized and applied in the photocatalytic water splitting for the first time. As illustrated in **Scheme 1**, the micron-sized three-way nitrogen-doped carbon tube (TNCT) was first prepared by a calcination method. Then, the MoS₂ nanosheets were loaded on the TNCT by a hydrothermal method. The as-prepared TNCT@MoS₂ composite exhibits much higher photocatalytic activities than pure MoS₂, which is ascribed to the improved charge separation and transfer efficiency afforded by the TNCT.

EXPERIMENTAL SECTION

Materials

Ammonium molybdate tetrahydrate, thiourea, ethanol, and terephthalic acid (TA) were supplied by China National Pharmaceutical Group Chemical Testing Co., Ltd. Melamine sponge is purchased from Zhengzhou Fengtai nanomaterial Co., Ltd. The water used in the experiment is secondary deionized water.

Preparation of TNCT

The commercial melamine sponge was calcined at 450°C for 3 h in vacuum, and the sponge changed from white to black. At this time, the required three-way nitrogen-doped carbon tube (TNCT) was initially formed.

Fabrication of TNCT@MoS₂

First, 1.24 g ammonium molybdate tetrahydrate, 2.26 g thiourea and 35 ml deionized water was mixed and stirred at room temperature for 20 min. Then, the mixture and the as-prepared black TNCT were transferred to a 100 mL polytetrafluoroethylene reactor. The reactor was heated in an

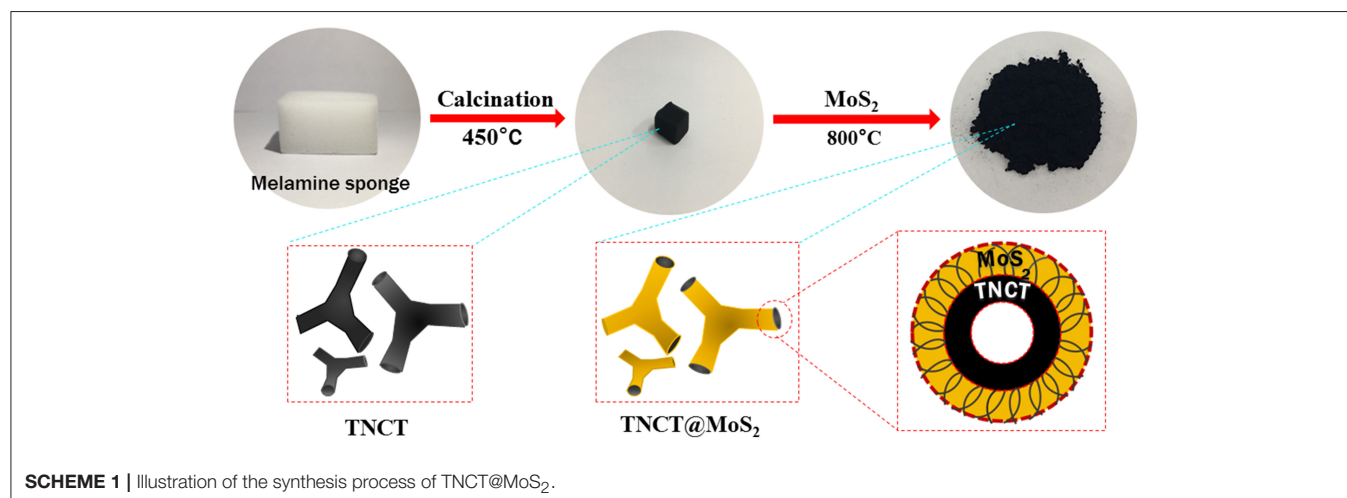
oven at 220°C for 24 h. After the reaction, the supernatant is poured off, and the sponge block is clamped out. After being mashed, the sponge block was centrifuged and washed with distilled water and ethanol for several times. Then, it was dried in a vacuum drying box at 60°C for 12 h, and a black powder was obtained. Finally, the black powder was calcined at 800°C in N₂ atmosphere for 4 h.

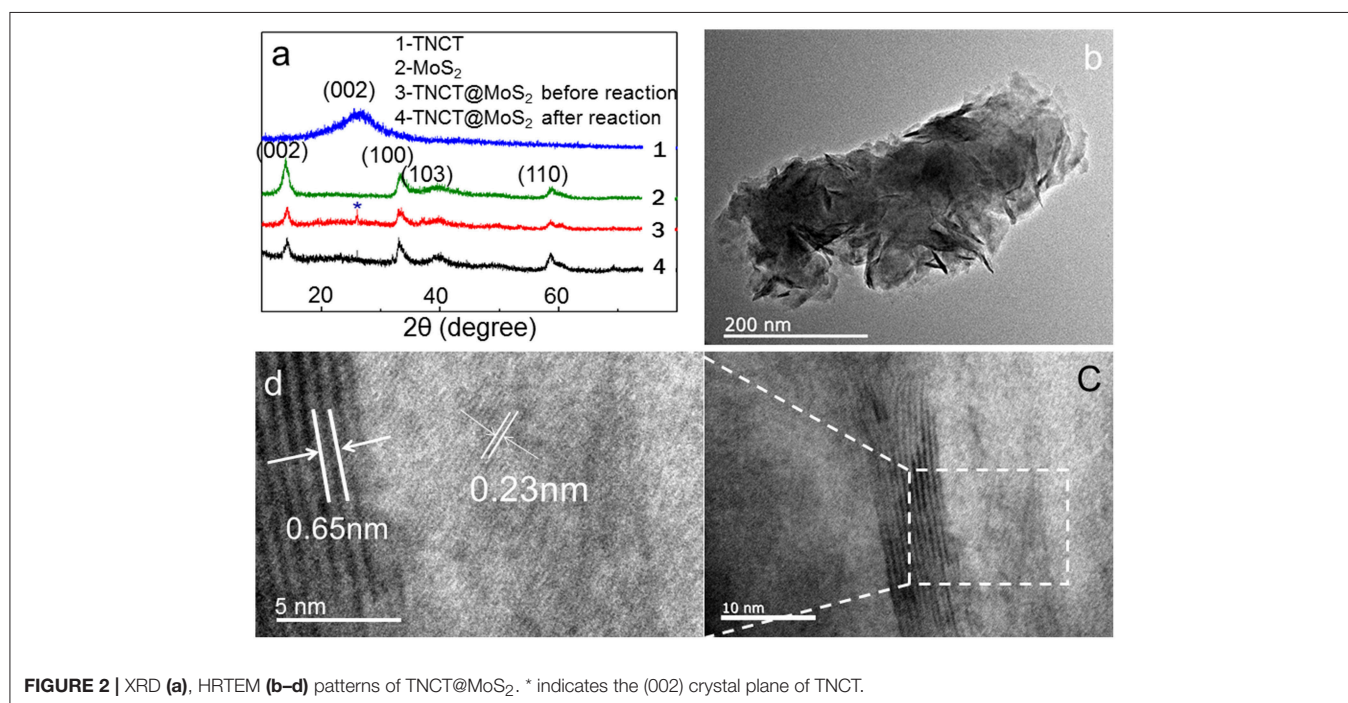
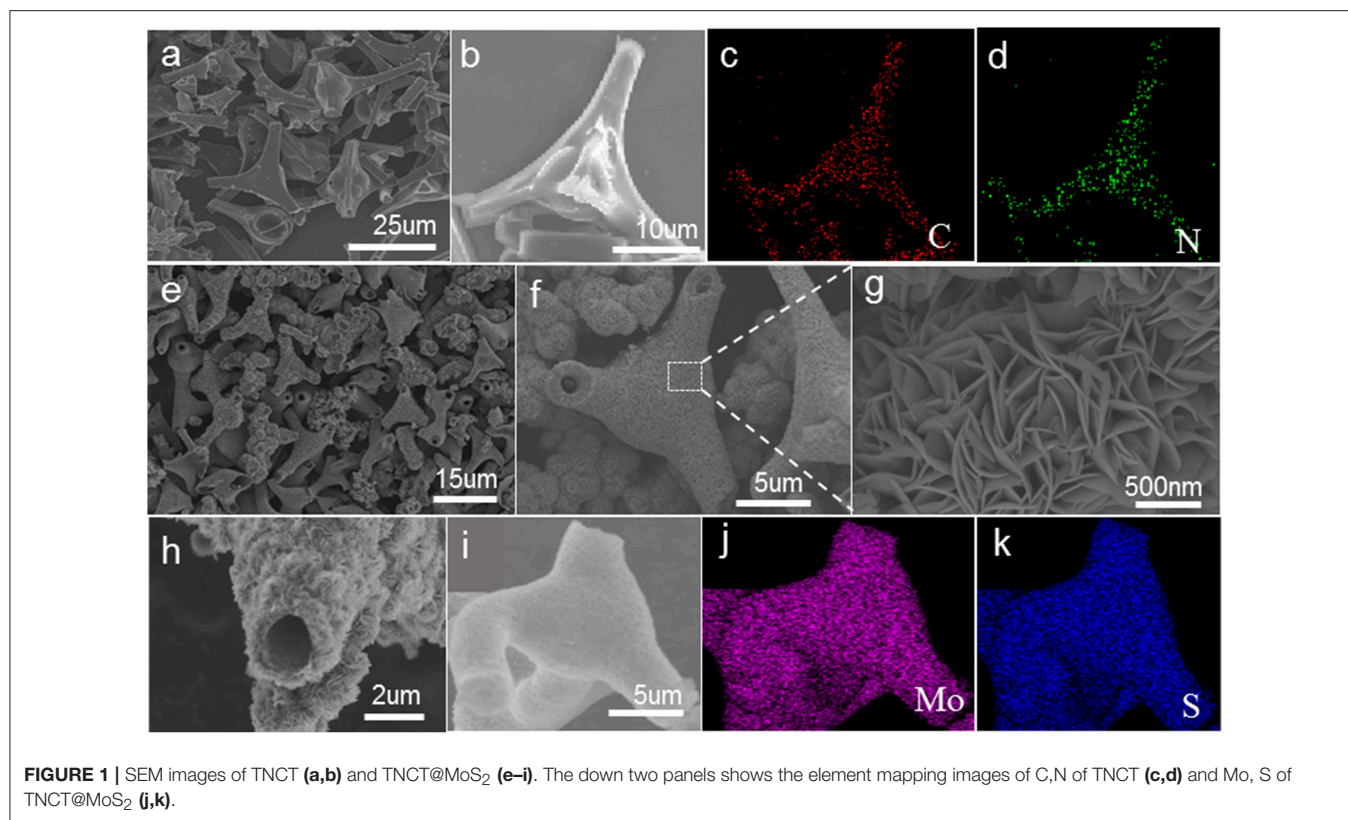
Instruments

Scanning Electron Microscope (SEM) equipped with a field-emission gun operated at 5.0 kV was used to characterize the morphology of the as-obtained product. High-Resolution Transmission Electron Microscopy (HRTEM) was taken on JEM-2100F instrument at an accelerating voltage of 200 kV. X-ray diffraction (XRD) analyses carried out on a Bruker D8 Advance Diffractometer with Cu K α radiation (1.5418 Å). X-ray photoelectron spectroscopy (XPS) was carried on Thermo Scientific Escalab 250Xi with Al K α as the excitation source. Photoelectrochemical performance measurements were performed in a standard three-electrode PEC cell, with three-way nitrogen-doped carbon tube@MoS₂, saturated calomel electrode, and Pt wire as the working electrode, reference electrode, and counter electrode, respectively. The fluorescence spectrum was carried out with an Edinburgh FLS920 spectrofluorimeter (Edinburgh Instruments Ltd, England) equipped with a xenon lamp. Raman spectra were measured by LabRAM HR800 confocal microscope Raman spectrometer from Horiba Jobin-Yvon, France. The UV/Vis diffuse reflection spectra (DRS) were taken on a Shimadzu UV-2550 spectrophotometer with an integrated sphere attachment and BaSO₄ used as the reference sample.

Photocatalytic Activity for Water Splitting

In a typical process, 20 mg of the as-prepared photocatalysts and 10 mL aqueous solution in a 20 mL Quartz bottle sealed with silicone rubber septum. Prior to photocatalysis experiment, the sample solutions were thoroughly deaerated by evacuation and purged with nitrogen for 10 min. Then it was irradiated





by a 1,000 W Xenon lamp (the light intensity irradiating the photocatalysts was 0.17 W) at room temperature under constant stirring. The produced gas was analyzed by gas chromatography (FULI 9750, TCD, Nitrogen as the carrier gas, and 5 Å molecular sieve column).

Because there was no O₂ detected in this photocatalytic water splitting system, to confirm the photocatalytic water splitting process, the intermediate OH directly photogenerated from water was determined as following (Yang et al., 2009). A fluorescence probe named terephthalic acid (TA) was

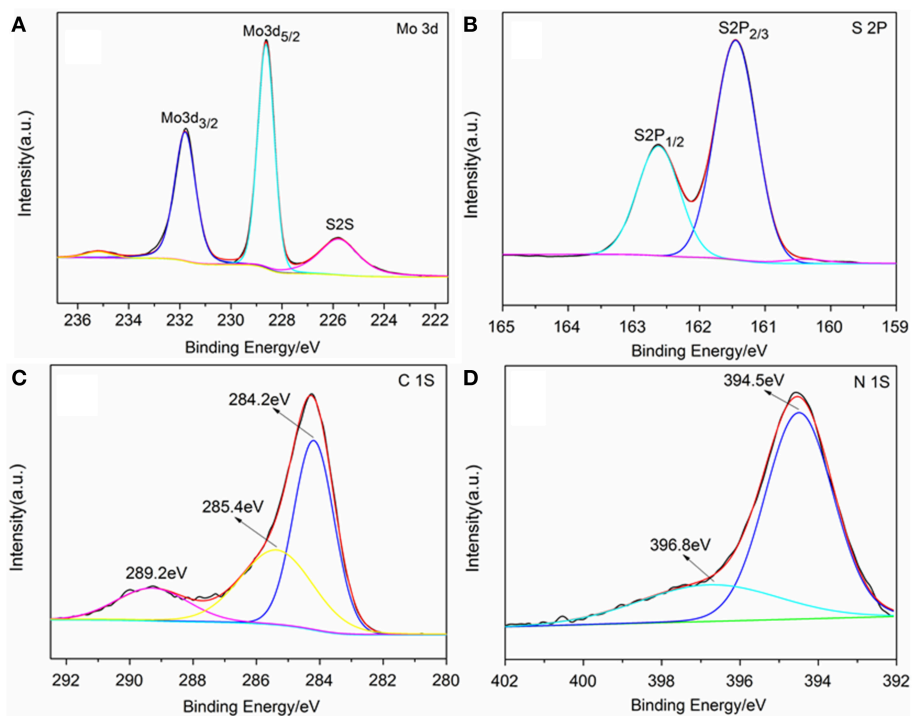


FIGURE 3 | XPS spectrum of TNCT@MoS₂. Mo 3d spectrum (A), S 2p spectrum (B), C 1s spectrum (C), and N 1s spectrum (D).

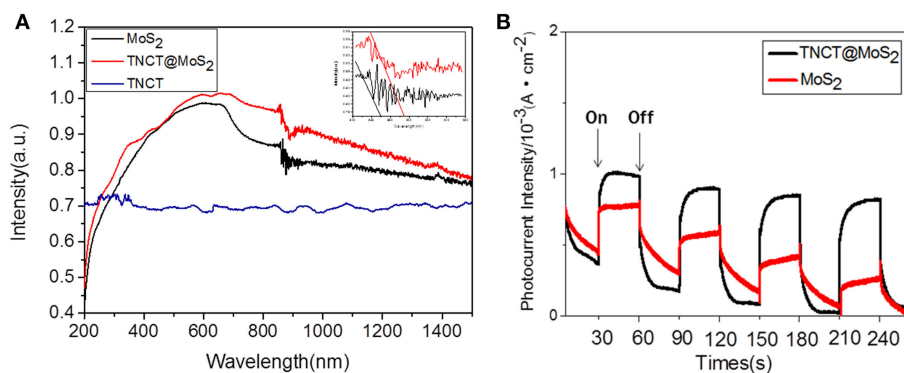
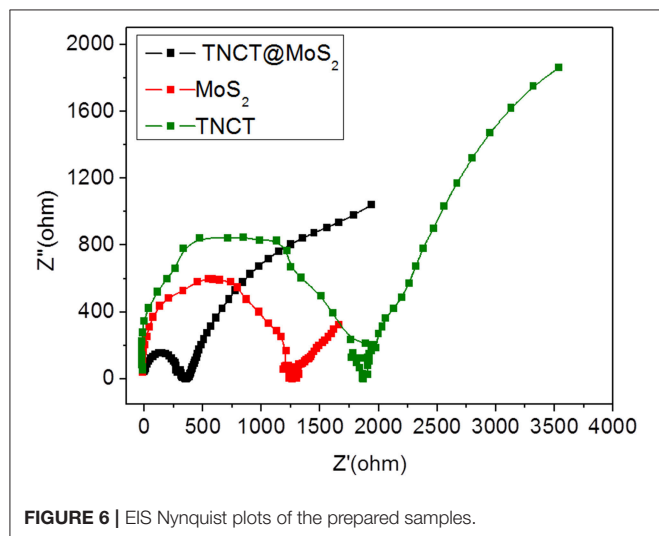
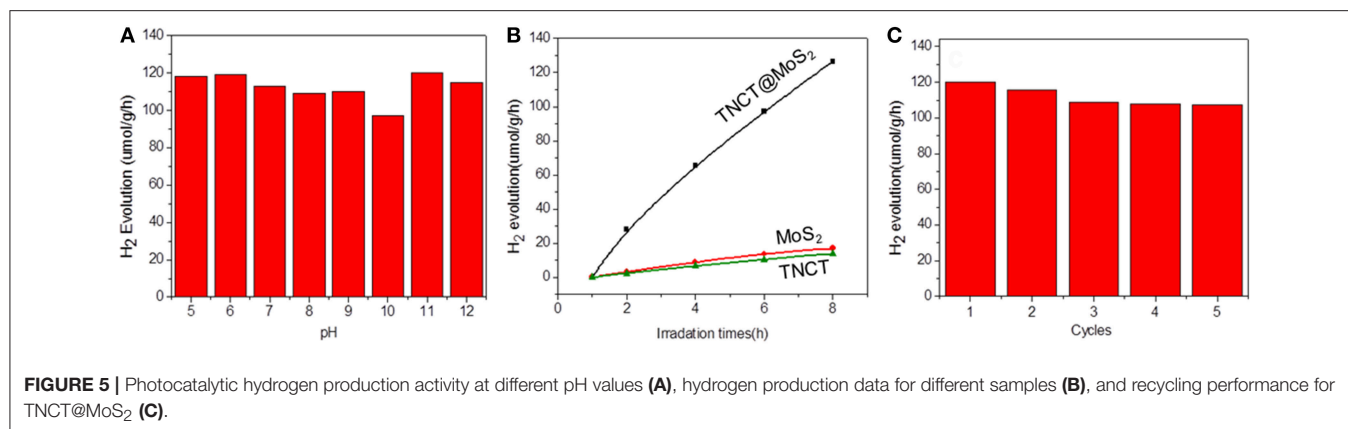


FIGURE 4 | UV-Vis-IR absorbance spectrum (A) and photocurrent of the samples (B).

added into the above-mentioned photocatalytic H₂ evolution measurement system to capture OH photogenerated from water, in a result of producing TAOH. Typically, 0.01M TA, 20 mg TNCT@MoS₂, and 10 mL water were mixed in a 20 mL Pyrex bottle at ambient temperature and atmospheric pressure, sealed with silicone rubber septum. The sample solutions were thoroughly deaerated by evacuation and argon bubbling for 2 h prior to photocatalysis experiment. Then it was irradiated by a 1,000-W Xe lamp under ambient conditions and magnetic stirring for certain time. The produced solutions containing TAOH were analyzed by fluorescence spectra.

RESULTS AND DISCUSSION

As shown in **Figures 1a,b**, most of these nitrogen-doped carbon tubes have three-way branches, each of which is about 20 microns in length and 3 micron in diameter. The EDS-mapping pictures show that the doped nitrogen elements are uniformly dispersed in the carbon tubes (**Figures 1c,d**). The SEM image of TNCT@MoS₂ heterostructures is shown in **Figures 1e-h**. It can be seen that the MoS₂ nanosheets layer with thickness of 500 nm are uniformly coated on the TNCTs. The MoS₂ nanosheets are interconnected with each other, forming the 2D nanosheets networks. Additionally, the EDS mapping pictures show that



MoS₂ nanosheets are uniformly dispersed on the surface of TNCT (Figures 1j,k).

XRD peaks of TNCT@MoS₂ localized at 2θ values of 13.8, 33.5, 39.8, and 58.8° are ascribed to MoS₂ with typical hexagonal phase (JCPDS:00-037-1492, Figure 2a). The (002) crystal plane diffraction peak is stronger than the diffraction peaks on other crystal planes, indicating that MoS₂ has a good layered packing structure (Zong et al., 2008). An obvious reflection located at $2\theta = 26.5^\circ$ is ascribed to the TNCT (002) crystal plane (Figure 2a; Tang et al., 2015). The heterogeneous lattice interfaces of MoS₂ and TNCT were clearly observed on the HRTEM images (Figures 2b,d). The lattice fringe spacing of 0.65 nm is ascribed to hexagonal phase MoS₂ (Choi et al., 2017). The lattice fringes of TNCT are not significant maybe due to the doping of nitrogen atoms, a dimly visible lattice spacing of 0.22 nm was ascribed to the (100) facet of graphite (Baker and Baker, 2010). The strong wide peaks located at 1,379 cm⁻¹ (D-band) in the Raman spectra showed that the presence and partial graphitization of carbon (Supplementary Figure 1; Matthews et al., 1999) in agreement with the results observed from the HRTEM images.

The chemical state of surface species of the samples was further determined by X-ray photoelectron spectroscopy (XPS).

The survey XPS spectra showed that Mo, S, N, C, and O elements existed in the surface layer of the as-prepared nanostructures (Supplementary Figure 2). Two peaks located at 228.62 and 231.79 eV are attributed to Mo 3d_{5/2} and Mo 3d_{3/2}, respectively (Figure 3B; Wang et al., 2017). The peak located at 161.8 eV corresponds to the S 2p_{3/2} and another one located at 162.7 eV was assigned to S 2p_{1/2} (Figure 3C; Hu et al., 2014). Three peaks were observed in the C 1s binding region peaks centered at 284.2, 285.4 and 289.2 eV, which were ascribed to graphite-C, -C*-C=O and -C* =O groups, respectively (Figure 3D; Christie et al., 1983; Beamson and Briggs, 1993; Wittek et al., 1996). Two peaks were observed in the N1s binding region peaks (Figure 3A). The peak centered at 394.5 eV indicated that the doped nitrogen in TNCT was connected with the carbon frame by -N* =N*-C bond (Kudo et al., 1986). It is worth noting that another peak for N1s centered at 396.8 eV was ascribed to Mo(-N* =N-)₂-C (George and Kwarcinski, 1995), which indicated that the MoS₂ could closely bond with TNCT by the surface -N=N- group.

The UV-Vis-IR absorbance spectrum shows that TNCT@MoS₂ exhibits higher and broader spectral absorption including IR light than that of TNCT and MoS₂ (Figure 4A). As shown in Figure 4B, TNCT@MoS₂ obviously shows higher photocurrent density than that of MoS₂. It indicates that TNCT@MoS₂ maybe has better photocatalytic activity.

The photocatalytic activity of the as-prepared catalyst was investigated for the photocatalytic water splitting process without addition of any sacrificial agents, which was performed by a 1,000 W xenon lamp source. It was found that the catalyst showed almost the same photocatalytic activity in the wide pH range of 5-11 and pure water (Figure 5A). The optimal hydrogen production rate of TNCT@MoS₂ was 120 μmol/g·h, which is about 9 times faster than that of pure MoS₂ (Figure 5B).

For a typical photocatalytic water splitting process, both H₂ and O₂ are usually produced from water. However, in this work, whereas this system readily produces hydrogen under illumination, the simultaneous liberation of oxygen is not observed. This phenomenon has been observed in much water splitting systems (Duonghong and Grätzel, 1984; Liu et al., 2012; Zhang et al., 2014). It is because the produced O₂ or intermediate oxygen species such as OH are readily absorbed by the metal elements such as Mo and W to form steady peroxide complexes,

in a result of inhibiting the release of O₂ (Cui et al., 2015). Herein, although there was no O₂ determined in this photocatalytic water splitting system, intermediate OH directly photogenerated from water was detected by the fluorescence probe TA (Yang et al., 2009). The fluorescence spectra of TAOH, which is produced through the oxidation of TA by OH, exhibited a peak at 426 nm, indicating the presence of OH (**Supplementary Figure 3**). Although the surface of molybdenum sulfide suffer from the produced intermediate active oxygen, the XRD (**Figure 2a**) and Raman spectroscopy (**Supplementary Figure 4**) showed that the crystal structure of the material did not change fundamentally and maintain the same photoactivity for five photocatalytic reaction runs (**Figure 5C**).

The excellent photocatalytic performance of TNCT@MoS₂ is ascribed to the effective separation and transfer of photogenerated carriers. Herein, it was verified by the photoluminescence spectroscopy and photoelectrochemical performance measurements. The photoluminescence (PL) of semiconductors was caused by recombination of photoinduced electrons and holes. If the recombination was suppressed, the PL emission of semiconductors would be quenched. As shown in **Supplementary Figure 5**, after being combined with TNCT, the PL intensity of MoS₂ emission peak obviously quenched. It indicated that the photoinduced charge separation efficiency of TNCT@MoS₂ would improve. The photogenerated carriers' transfer capacity of the as prepared materials was confirmed by electrochemical impedance tests. As shown in **Figure 6**, TNCT, MoS₂, and TNCT@MoS₂ all showed classical semicircular Nyquist diagram. The arc radius of TNCT@MoS₂ was obviously smaller than that of TNCT and MoS₂, which indicated that the photogenerated charges in TNCT@MoS₂ would suffer less resistance. It is ascribed to the fast charge transfer from MoS₂ nanosheets to carbon tube under full-light irradiation. The formed Mo(-N* =N-)₂-C bonding connection between MoS₂ and TNCT maybe acts as carrier transfer bridge (**Figure 3D**), which will improve the photogenerated carriers separation and transfer efficiency of TNCT@MoS₂. The detailed mechanism and remained questions would be studied in our future work.

REFERENCES

- Anna, M.-M., Lluís, S., Miquel, T., Pol, S., Jordi, L., and Anna, R. (2018). Fast and Simple Microwave synthesis of TiO₂/Au nanoparticles for gas-phase photocatalytic hydrogen generation. *Front Chem.* 6:110. doi: 10.3389/fchem.2018.00110
- Baker, S. N., and Baker, G. A. (2010). Luminescent carbon nanodots: emergent nanolights. *Angew. Chem. Int. Ed.* 49, 6726–6744. doi: 10.1002/chin.201103270
- Beamson, G., and Briggs, D. (1993). High resolution XPS of organic polymers: the scienta ESCA300 database. *J. Chem. Educ.* 70:A25 doi: 10.1021/ed070pA25.5
- Chang, K., Mei, Z. W., Wang, T., Kang, Q., Ouyang, S. X., and Xe, J. H. (2014). MoS₂/graphene cocatalyst for efficient photocatalytic H₂ evolution under visible light irradiation. *ACS Nano.* 8, 7078–7087. doi: 10.1021/nn5019945
- Cheiwchanchamngij, T., and Lambrecht, W. R. L. (2012). Quasiparticle band structure calculation of monolayer, bilayer, and bulk MoS₂. *Phys. Rev. B.* 85:205302. doi: 10.1103/PhysRevB.85.205302
- Chen, X., Zhang, W. J., Tang, J. T., Pan, C. Y., and Yu, G. P. (2018). Porous organic polymers: an emerged platform for photocatalytic water splitting. *Front Chem.* 6:592. doi: 10.3389/fchem.2018.00592

CONCLUSIONS

In summary, a micron-sized three-way nitrogen-doped carbon tube covered with MoS₂ nanosheets was synthesized and applied in the photocatalytic water splitting without any sacrificial agents for the first time. The micron-sized three-way nitrogen-doped carbon tube is facilely synthesized by the calcination of sponge at 450°C in vacuum. And then the MoS₂ nanosheets are deposited on the three-way nitrogen-doped carbon tubes by a simple hydrothermal method. Compared with MoS₂, the TNCT@MoS₂ heterostructures showed higher H₂ evolution rate, which may be ascribed to the improved charge separation and transfer efficiency caused by the three-way nitrogen-doped carbon tube. This work may provide a new design idea for the design of low-cost and efficient photocatalysts.

AUTHOR CONTRIBUTIONS

GC and BT conceived and designed the experiments. YuZ, YL, PC, HC, and YF performed the experiments. WG, XS, and YiZ analyzed the data. GC and YuZ co-wrote the paper.

FUNDING

This work was supported by the National Natural Science Foundation of China (21535004, 91753111, 21575082, 21775092, 21507074) and the Key Research and Development Program of Shandong Province (2018YFJH0502), Development plan of science and technology for Shandong Province of China (2013GGX10706), Shandong Province Natural Science Foundation (ZR2015BM023, ZR2018JL008), and the Project of Shandong Province Higher Educational Science and Technology Program (J13LD06).

SUPPLEMENTARY MATERIAL

The Supplementary Material for this article can be found online at: <https://www.frontiersin.org/articles/10.3389/fchem.2019.00325/full#supplementary-material>

- Cheng, J. S., Zhao, H., Kangle, L., Wu, X. F., Li, Q., Li, Y. H., et al. (2018). Drastic promoting the visible photoreactivity of layered carbon nitride by polymerization of dicyandiamide at high pressure. *Appl. Catal. B Environ.* 232, 330–339. doi: 10.1016/j.apcatb.2018.03.066
- Cheng, J. S., Zhao, H., Li, Q., Li, X. F., Fang, S., Wu, X. F., et al. (2019). Fabrication of high photoreactive carbon nitride nanosheets by polymerization of amidinourea for hydrogen production. *Appl. Catal. B Environ.* 245, 197–206. doi: 10.1016/j.apcatb.2018.12.044
- Choi, J., Reddy, D. A., Han, N. S., Jeong, S., Hong, S., Kumar, D. P., et al. (2017). Modulation of charge carrier pathways in CdS nanospheres by integrating MoS₂ and Ni₂P for improved migration and separation toward enhanced photocatalytic hydrogen evolution. *Catal. Sci. Technol.* 7, 641–649. doi: 10.1039/c6cy02145j
- Christie, A. B., Lee, J., Sutherland, I., and Walls, J. M. (1983). An XPS study of ion-induced compositional changes with group II and group IV compounds. *Appl. Surf. Sci.* 15, 224–237. doi: 10.1016/0378-5963(83)90018-1
- Cui, G.-W., Wang, W.-L., Ma, M.-Y., Zhang, M., Xia, X.-Y., Han, F.-Y., et al. (2013). Rational design of carbon and TiO₂ assembly materials: covered or

- strewn, which is better for photocatalysis? *Chem. Commun.* 49, 6415–6417. doi: 10.1039/c3cc42500b
- Cui, G. W., Wang, W., Ma, M. Y., Xie, J. F., Shi, X. F., Deng, N., et al. (2015). IR-driven photocatalytic water splitting with WO₂-Na₂WO₃ hybrid conductor material. *Nano Lett.* 15, 7199–7203. doi: 10.1021/acs.nanolett.5b01581
- Dong, S., Sun, J., Li, Y., Yu, C., Li, Y., and Sun, J. (2013). ZnSnO₃ hollow nanospheres/reduced graphene oxide nanocomposites as high-performance photocatalysts for degradation of metronidazole. *Appl. Catal. B* 144, 386–393. doi: 10.1016/j.apcatb.2013.07.043
- Duonghong, D., and Grätzel, M. (1984). Colloidal TiO₂ particles as oxygen carriers in photochemical water cleavage systems. *J. Chem. Soc. Chem. Commun.* 1597–1599. doi: 10.1039/C39840001597
- George, T. A., and Kwarcinski, M. E. (1995). Preparation and properties of diazenido, hydrazido(2-), and hydrido-hydrazido(2-) complexes of tungsten. x-ray photoelectron spectroscopy of dinitrogen and hydrazido(2-) complexes of molybdenum and tungsten. *J. Coord. Chem.* 35, 349–357. doi: 10.1080/00958979508024047
- Guo, X., Cao, G.-L., Ding, F., Li, X. Y., Zhen, S. Y., Xue, Y.-F., et al. (2015). A bulky and flexible electrocatalyst for efficient hydrogen evolution based on the growth of MoS₂ nanoparticles on carbon nanofiber foam. *J. Mater. Chem. A* 3, 5041–5046. doi: 10.1039/c5ta00087d
- Hinnemann, B., Moses, P. G., Bonde, J., Jørgensen, K. P., Nielsen, J. H., Horch, S., et al. (2005). Biomimetic hydrogen evolution: MoS₂ nanoparticles as catalyst for hydrogen evolution. *J. Am. Chem. Soc.* 127, 5308–5309. doi: 10.1021/ja0504690
- Hu, S., Chen, W., Zhou, J., Yin, Y., Uchaker, E., Zhang, Q. F., et al. (2014). Preparation of carbon coated MoS₂ flower-like nanostructure with self-assembled nanosheets as high-performance lithium-ion battery anodes. *J. Mater. Chem. A* 2, 7862–7872. doi: 10.1039/c4ta01247j
- Jia, T. T., Kolpin, A., Ma, C. S., Chan, R. C.-T., Kwok, W. M., and Tsang, S. C. E. (2013). A graphene dispersed CdS–MoS₂ nanocrystal ensemble for cooperative photocatalytic hydrogen production from water. *Chem. Commun.* 50, 1185–1188. doi: 10.1039/c3cc47301e
- Jiang, Y.-R., Lee, W., Chen, K.-T., Wang, M.-C., Chang, K.-H., and Chen, C.-C. (2013). Hydrothermal synthesis of b-ZnMoO₄ crystals and their photocatalytic degradation of Victoria Blue R and phenol. *J. Taiwan Inst. Chem. Eng.* 45, 207–218. doi: 10.1016/j.jtice.2013.05.007
- Kudo, Y., Yoshida, N., Fujimoto, M., Tanaka, K., and Toyoshima, I. (1986). Acid-dissociation behavior of para-hydroxyl group in the N₃N₂O-terdentate ligand, 4-(4-methyl-2-pyridylazo)resorcinol, coordinated to a transition metal ion. *Bull. Chem. Soc. Jpn.* 59, 1481–1486. doi: 10.1246/bcsj.59.1481
- Lang, D., Shen, T. T., and Xiang, Q. J. (2015). Roles of MoS₂ and graphene as cocatalysts in the enhanced visible-light photocatalytic H₂ production activity of multiarmed CdS nanorods. *Chemcatchem* 7, 943–951. doi: 10.1002/cctc.201403062
- Liu, J. H., Zhang, Y. W., Lu, L. H., Wu, G., and Wei, C. (2012). Self-regenerated solar-driven photocatalytic water-splitting by urea derived graphitic carbon nitride with platinum nanoparticles. *Chem. Commun.* 48, 8826–8828. doi: 10.1039/C2CC33644H
- Marchal, C., Cottineau, T., Méndez-Medrano, M. G., Colbeau-Justin, C., Caps, V., and Keller, V. (2018). Au/TiO₂-g-C₃N₄ nanocomposites for enhanced photocatalytic H₂ production from water under visible light irradiation with very low quantities of sacrificial agents. *Adv. Energy Mater.* 8:1702142. doi: 10.1002/aenm.201702142
- Matthews, M. J., Pimenta, M. A., Dresselhaus, G., et al. (1999). Origin of dispersive effects of the raman d band in carbon materials. *Physical Review B* 59:R6585. doi: 10.1103/PhysRevB.59.R6585
- Pan, H. (2016). Principles on design and fabrication of nanomaterials as photocatalysts for water-splitting. *Renew. Sustain. Energy Rev.* 57, 584–601. doi: 10.1016/j.rser.2015.12.117
- Pan, Y., Lin, Y., Liu, Y. Q., and Liu, C. G. (2016). A novel CoP/MoS₂-CNTs hybrid catalyst with Ptlike activity for hydrogen evolution. *Catal. Sci. Technol.* 6, 1611–1615. doi: 10.1039/c5cy02299a
- Shao, M. M., Shao, Y. F., Chai, J. W., Qu, Y. J., Yang, M. Y., Wang, Z. L., et al. (2017). Synergistic effect of 2D Ti₂C and g-C₃N₄ for efficient photocatalytic hydrogen production. *J. Mater. Chem. A* 5, 16748–16756. doi: 10.1039/c7ta04122e
- Shao, M. M., Shao, Y. F., Ding, S. J., Wang, J. W., Xu, J. C., Qu, Y. J., et al. (2018). Vanadium disulfide decorated graphitic carbon nitride for super-efficient solar-driven hydrogen evolution. *Appl. Catal. B Environ.* 237, 295–301. doi: 10.1016/j.apcatb.2018.05.084
- Shi, T., Duan, Y., Lv, K., Hu, Z., Li, Q., Li, M., et al. (2018). Photocatalytic oxidation of acetone over high thermally stable TiO₂ nanosheets with exposed (001) facets. *Front Chem.* 6:175. doi: 10.3389/fchem.2018.00175
- Tang, J., Salunkhe, R. R., Liu, J., Torad, N. L., Imura, M., Furukawa, S., et al. (2015). Thermal conversion of core-shell metal-organic frameworks: a new method for selectively functionalized nanoporous hybrid carbon. *J. Am. Chem. Soc.* 137, 1572–1580. doi: 10.1021/ja511539a
- Wang, J. Z., Dong, S. Y., Guo, T., Jin, J., and Sun, J. H. (2017). pH-dictated synthesis of novel flower-like MoS₂ with augmented natural sunlight photocatalytic activity. *Mater. Lett.* 191, 22–25. doi: 10.1016/j.matlet.2016.12.090
- Wang, L. J., Fan, J., Cao, Z., Zheng, Y., Yao, Z., Shao, G., et al. (2014). Fabrication of predominantly Mn⁴⁺-doped TiO₂ nanoparticles under equilibrium conditions and their application as visible-light photocatalysts. *Chem Asian. J.* 9, 1904–1912. doi: 10.1002/asia.201402114
- Wang, L. J., Zhang, X., Gao, H. Q., Hu, J. H., Mao, J., Liang, C. H., et al. (2016). 3D CuO network supported TiO₂ nanosheets with applications for energy storage and water splitting. *Sci. Adv. Mater.* 8, 1256–1262. doi: 10.1166/sam.2016.2714
- Wang, Q. S., Wen, Y., Cai, K. M., Cheng, R. Q., Yin, L., Zhang, Y., et al. (2018). Nonvolatile infrared memory in MoS₂/PbS van der Waals heterostructures. *Sci. Adv.* 4:eaap7916. doi: 10.1126/sciadv.aap7916
- Witek, G., Noeske, M., Mestl, G., Shaikhutdinov, S., and Behm, R. J. (1996). Interaction of platinum colloids with single crystalline oxide and graphite substrates: a combined AFM, STM and XPS study. *Catal. Lett.* 37, 35–39. doi: 10.1007/BF00813516
- Wolff, C. M., Frischmann, P. D., Schulze, M., Bohn, B. J., Wein, B., Livadas, P., et al. (2018). All-in-one visible-light-driven water splitting by combining nanoparticulate and molecular co-catalysts on CdS nanorods. *Nat. Energy.* 3, 862–869. doi: 10.1038/s41560-018-0229-6
- Xiang, Q. J., Yu, J. G., and Jaroniec, M. (2012). Synergetic effect of MoS₂ and graphene as cocatalysts for enhanced photocatalytic H₂ production activity of TiO₂ nanoparticles. *J. Am. Chem. Soc.* 134, 6575–6578. doi: 10.1021/ja302846n
- Yang, C., Li, Q., Xia, Y., Lv, K., and Li, M. (2019). Enhanced visible-light photocatalytic CO₂ reduction performance of ZnIn₂S₄ microspheres by using CeO₂ as cocatalyst. *Appl. Surf. Sci.* 464, 388–395. doi: 10.1016/j.apsusc.2018.09.099
- Yang, H. G., Liu, G., Qiao, S. Z., Sun, C. H., Jin, Y. G., Smith, S. C., et al. (2009). Solvothermal synthesis and photoreactivity of anatase TiO₂ nanosheets with dominant {001} facets. *J. Am. Chem. Soc.* 131, 4078–4083. doi: 10.1021/ja808790p
- Zeng, D., Xu, W., Ong, W.-J., Xu, J., Ren, H., Chen, Y., et al. (2018). Toward noble-metal-free visible-light-driven photocatalytic hydrogen evolution: monodisperse sub-15 nm Ni₂P nanoparticles anchored on porous g-C₃N₄ nanosheets to engineer 0D-2D heterojunction interfaces. *Appl. Catal. B* 221, 47–55. doi: 10.1016/j.apcatb.2017.08.041
- Zhang, M., Respinis, M. D., and Frei, H. (2014). Time-resolved observations of water oxidation intermediates on a cobalt oxide nanoparticle catalyst. *Nat. Chem.* 6, 362–367. doi: 10.1038/nchem.1874
- Zong, X., Yan, H. J., Wu, G. P., Ma, G. J., Wen, F. Y., Wang, L., et al. (2008). Enhancement of photocatalytic H₂ evolution on CdS by loading MoS₂ as cocatalyst under visible light irradiation. *J. Am. Chem. Soc.* 130, 7176–7177. doi: 10.1021/ja8007825

Conflict of Interest Statement: The authors declare that the research was conducted in the absence of any commercial or financial relationships that could be construed as a potential conflict of interest.

Copyright © 2019 Zhang, Liu, Gao, Chen, Cui, Fan, Shi, Zhao, Cui and Tang. This is an open-access article distributed under the terms of the Creative Commons Attribution License (CC BY). The use, distribution or reproduction in other forums is permitted, provided the original author(s) and the copyright owner(s) are credited and that the original publication in this journal is cited, in accordance with accepted academic practice. No use, distribution or reproduction is permitted which does not comply with these terms.